Inorganic Chemistry
Cite This: Inorg. Chem. XXXX, XXX, XXX–XXX
Article
pubs.acs.org/IC

Photochemotherapeutic Properties of a Linear Tetrapyrrole Palladium(II) Complex displaying an Exceptionally High Phototoxicity Index

Andrea M. Potocny,[†,⊥] Rachel S. Riley,[‡,⊥] Rachel K. O'Sullivan,[‡] Emily S. Day,[*,‡,§,∥] and Joel Rosenthal[*,†]

[†]Department of Chemistry and Biochemistry, [‡]Department of Biomedical Engineering, and [§]Department of Materials Science and Engineering, University of Delaware, Newark, Delaware 19716, United States

[∥]Helen F. Graham Cancer Center and Research Institute, Newark, Delaware 19713, United States

Supporting Information

ABSTRACT: Photodynamic therapy (PDT) represents a minimally invasive and highly localized treatment strategy to ablate tumors with few side effects. In PDT, photosensitizers embedded within tumors are activated by light and undergo intersystem crossing, followed by energy transfer to molecular oxygen, resulting in the production of toxic singlet oxygen ($^1O_2$). Previously, we reported a robust, linear tetrapyrrole palladium(II) complex, **Pd[DMBil1]**, characterized by its facile and modular synthesis, broad absorption profile, and efficient $^1O_2$ quantum yield of Φ_Δ = 0.8 in organic media. However, the insolubility of this porphyrinoid derivative in aqueous solution prevents its use under biologically relevant conditions. In this work, we report the synthesis of **Pd[DMBil1]-PEG$_{750}$**, a water-soluble dimethylbiladiene derivative that is appended with a poly(ethylene) glycol (PEG) functionality. Characterization of this complex shows that this PEGylated biladiene architecture maintains the attractive photophysical properties of the parent complex under biologically relevant conditions. More specifically, the absorption profile of **Pd[DMBil1]-PEG$_{750}$** closely matches that of **Pd[DMBil1]** and obeys the Beer–Lambert Law, suggesting that the complex does not aggregate under biologically relevant conditions. Additionally, the emission spectrum of **Pd[DMBil1]-PEG$_{750}$** retains the fluorescence and phosphorescence features characteristic of **Pd[DMBil1]**. Importantly, the PEGylated photosensitizer generates $^1O_2$ with Φ_Δ = 0.57, which is well within the range to warrant interrogation as a potential PDT agent for treatment of cancer cells. The **Pd[DMBil1]-PEG$_{750}$** is biologically compatible, as it is taken up by MDA-MB-231 triple negative breast cancer (TNBC) cells and has an effective dose (ED_{50}) of only 0.354 μM when exposed to λ_{ex} > 500 nm light for 30 min. Impressively, the lethal dose (LD_{50}) of **Pd[DMBil1]-PEG$_{750}$** without light exposure was measured to be 1.87 mM, leading to a remarkably high phototoxicity index of ~5300, which is vastly superior to existing photosensitizers that form the basis for clinical PDT treatments. Finally, through flow cytometry experiments, we show that PDT with **Pd[DMBil1]-PEG$_{750}$** induces primarily apoptotic cell death in MDA-MB-231 cells. Overall these results demonstrate that **Pd[DMBil1]-PEG$_{750}$** is an easily prepared, biologically compatible, and well-tolerated photochemotherapeutic agent that can efficiently drive the photoinduced apoptotic death of TNBC cells.

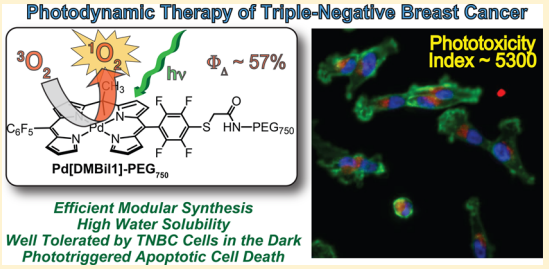

INTRODUCTION

Photodynamic therapy (PDT) is used clinically as a non-invasive treatment for solid tumors. In PDT, photosensitizing compounds are either intratumorally or intraveneously injected and circulate throughout the body prior to irradiation of the tumor site.[1] Photosensitizers present within the illuminated tissue absorb light and transfer energy to ground-state molecular oxygen to produce toxic $^1O_2$ that ultimately induces localized cell death (Scheme 1). PDT is regarded as a promising treatment strategy for certain types of cancers[2] and skin conditions,[3] because it is less invasive than surgical removal,[4] has fewer side effects than radiation or chemotherapy,[5−9] and can, in some cases, stimulate an antitumor immune response.[10,11]

Several photosensitizers, most of which belong to the porphyrinoid family of macrocyclic tetrapyrroles, have been approved for use in PDT.[12−14] However, widespread clinical use of PDT has been hindered, at least in part, because existing $^1O_2$ photosensitizers lack the photophysical and pharmacological attributes required for an optimal phototherapeutic agent. An ideal photosensitizer would be simple to synthesize and purify, demonstrate strong absorption of 600−850 nm light, which can penetrate deeper into tissues, and generate $^1O_2$ with a high quantum yield during irradiation. It is also critical that a photosensitizer for PDT be relatively nontoxic in the absence of light to minimize off-target side effects. Lastly, water

Received: May 4, 2018

DOI: 10.1021/acs.inorgchem.8b01225
Inorg. Chem. XXXX, XXX, XXX–XXX

Scheme 1. Photodynamic Therapy[a]

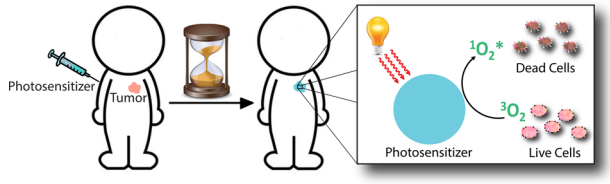

[a]Photosensitizers are intravenously or intratumorally administered. The tumor area is then irradiated, driving the formation of toxic $^1O_2$ to irreversibly damage/kill the surrounding cells.

solubility is critical to ensure stability during storage or intravenous injection and to prevent aggregation-induced attenuation of the $^1O_2$ quantum yield.

We recently demonstrated that the linear tetrapyrrole metal complex palladium 10,10-dimethyl-5,15-bis-(pentafluorophenyl)biladiene (**Pd[DMBil1]**, structure shown in Scheme 2) is capable of absorbing light up to $\lambda \approx 600$ nm and sensitizing $^1O_2$ with a high quantum yield ($\Phi_\Delta \approx 0.8$) that is on par with those of photosensitizers currently used in PDT.[15] Importantly, **Pd[DMBil1]** is easily synthesized in four steps from commercially available starting materials,[15] and it can be purified and isolated using modular methods. While these traits suggest that the **Pd[DMBil1]** core is well-suited for interrogation as a PDT agent, this compound's complete lack of water solubility has precluded such studies.

The addition of poly(ethylene) glycol (PEG) substituents is commonly employed in the development of therapeutics, since PEGs generally show excellent biocompatibility and lend high water solubility.[16−19] In the present study, we modified the **Pd[DMBil1]** photosensitizer with a PEG functionality to overcome the inherent hydrophobicity of the biladiene architecture. We demonstrate that the addition of this PEG functionality endows the dimethylbiladiene complex with water solubility while having little effect on its photophysical properties, thus generating a biocompatible compound, **Pd[DMBil1]-PEG$_{750}$**, that retains the ability to generate $^1O_2$ with a high quantum yield under biologically relevant conditions. Additionally, we demonstrate that, while this biladiene complex is highly nontoxic in the dark, it can serve as an extremely potent chemotherapeutic agent for treatment of triple negative breast cancer (TNBC) cells and drives apoptotic cell death with a remarkable phototoxicity index of ~5300.

RESULTS AND DISCUSSION

Pd[DMBil1]-PEG$_{750}$ is readily accessible from unfunctionalized **Pd[DMBil1]**, which is readily prepared (Scheme 2) in four steps using methodology previously developed for the synthesis of biladienes[15,20] and related tetrapyrroles containing sp^3 hybridized *meso*-carbons.[21−23] PEGylation of the parent **Pd[DMBil1]** architecture was facilitated by the presence of the two pentafluorophenyl substituents at the 5- and 15-positions, which can be derivatized via nucleophilic aromatic substitution of the *para*-fluorine substituents.[24−26] As shown in Scheme 2, treatment of **Pd[DMBil1]** with mercaptoacetic acid and NEt$_3$ at 90 °C in dimethylformamide (DMF) for 1 h afforded the monomercaptoacetic acid-substituted product (**Pd[DMBil]-SCH$_2$CO$_2$H**) in better than 75% yield following purification by flash chromatography. PEGylation of **Pd[DMBil]-SCH$_2$CO$_2$H** was achieved through conversion of the mercaptoacetic acid substituent into an *N*-(methoxyPEG)mercaptoacetamide using carbodiimide coupling chemistry.[27,28] **Pd[DMBil]-SCH$_2$CO$_2$H** was initially reacted with *N*-hydroxysuccinimide (NHS) and 1-ethyl-3-(3′-dimethylaminopropyl)carbodiimide hydrochloride (EDC) to form an NHS mercaptoacetate intermediate. Further treatment with triethylamine and a methoxy-PEG-amine with an average molecular weight of 750 Da resulted in the formation of **Pd[DMBil1]-PEG$_{750}$**, as is shown in Scheme 2. Detailed synthetic procedures and characterization data for all new compounds shown in Figure 2 are detailed in the Supporting Information.

The visible absorption profile of **Pd[DMBil1]-PEG$_{750}$** has three features centered at 402, 483, and 540 nm in methanol (Figure 1 and Table 1). Aside from showing a slight enhancement of the feature at 483 nm, this absorption profile is nearly identical to that of **Pd[DMBil1]** in methanol, suggesting that introduction of the thioether and PEG chain at the para position of one biladiene C_6F_5 substituent has little effect on the electronic structure of the palladium tetrapyrrole core. In a pH 7.4 phosphate-buffered saline (PBS) solution the

Scheme 2. Synthesis of Pd[DMBil1], Pd[DMBil1]-SCH$_2$CO$_2$H, and Pd[DMBil1]-PEG$_{750}$

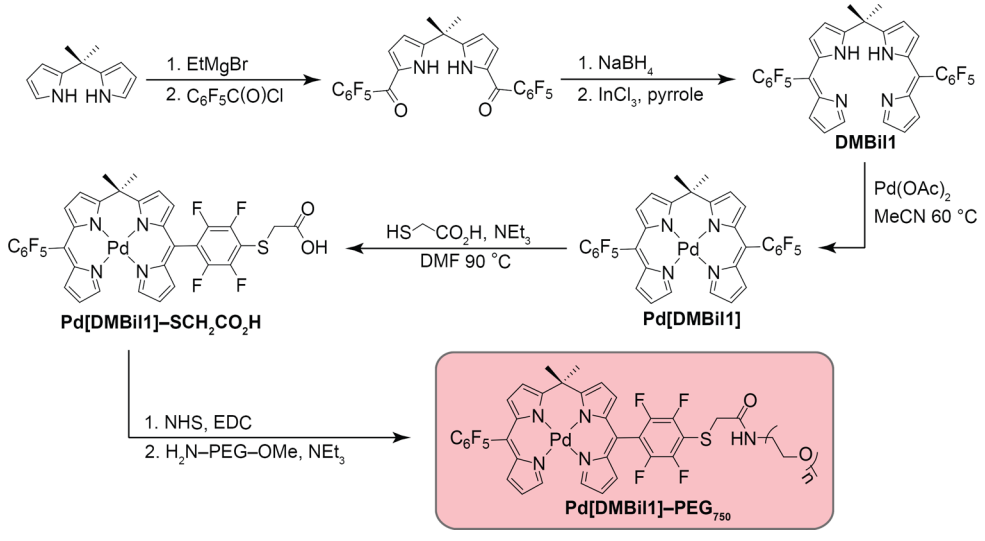

DOI: 10.1021/acs.inorgchem.8b01225
Inorg. Chem. XXXX, XXX, XXX−XXX

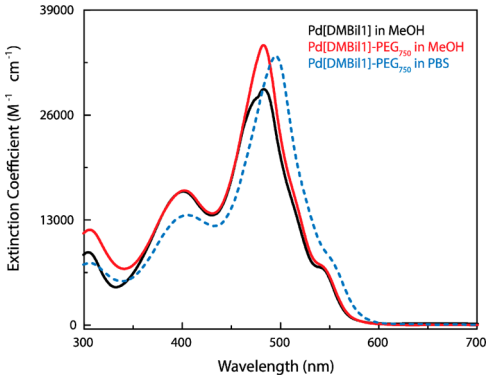

Figure 1. Electronic absorption spectra of **Pd**[**DMBil1**] in methanol (black line), **Pd**[**DMBil1**]-**PEG**$_{750}$ in methanol (red line), and **Pd**[**DMBil1**]-**PEG**$_{750}$ in pH 7.4 PBS (dashed blue line).

Table 1. Photophysical Properties of Pd[DMBil] Complexes

compound (solvent)	λ_{abs}, nm ($\varepsilon \times 10^3$ M^{-1} cm^{-1})	λ_{fl}, nm (Φ_{fl})	λ_{ph}, nm (Φ_{ph})	Φ_{Δ}[a]
Pd[**DMBil1**] (methanol)	401 (17.4), 483 (31.9), 540 (7.5)	557 (1.3×10^{-4})	753 (1.3×10^{-4})	0.80
Pd[**DMBil1**]-**PEG**$_{750}$ (methanol)	402 (16.6), 483 (34.6), 540 (7.5)	568 (1.4×10^{-4})	756 (7.8×10^{-5})	0.57
Pd[**DMBil1**]-**PEG**$_{750}$ (PBS)	405 (13.6), 496 (33.2), 551 (8.3)	580 (2.0×10^{-4})		0.23

[a]Measured upon irradiation with λ_{exc} = 500 nm.

absorption spectrum of **Pd**[**DMBil1**]-**PEG**$_{750}$ shows a bathochromic shift relative to its appearance in methanol. Although the full width at half-maximum (fwhm) of the most prominent absorption feature of the PEGylated derivative increases slightly from 63 nm in methanol to 67 nm in PBS, both of these values are smaller than the fwhm of the corresponding absorption feature of **Pd**[**DMBil1**] in methanol (73.5 nm). Furthermore, solutions of **Pd**[**DMBil1**]-**PEG**$_{750}$ behave in accordance with the Beer–Lambert Law when dissolved in either methanol or PBS at concentrations ranging from 4 to 24 μM (Supporting Information Figure S2). Self-aggregation of other tetrapyrroles under aqueous conditions has been associated with broadened absorption features[29−31] and deviations from the Beer–Lambert Law,[32] so the observation that **Pd**[**DMBil1**]-**PEG**$_{750}$ does not exhibit such behavior indicates that aggregation for this system should be insignificant. The **Pd**[**DMBil1**]-**PEG**$_{750}$ complex is also resistant to photodegradation, as the UV–vis absorption spectrum for this construct in PBS (24.0 μM) showed no substantial changes over the course of 2 h of irradiation with 500 or 550 nm light (Figure S3).

The emission properties of the **Pd**[**DMBil1**] complex in nitrogen-saturated methanol are also largely unaffected by PEGylation. As has been previously observed for **Pd**[**DMBil1**],[15] excitation of **Pd**[**DMBil1**]-**PEG**$_{750}$ with 500 nm light elicits weak fluorescence from 500 to 700 nm as well as phosphorescence from 700 to 850 nm (Figure 2). Table 1 shows that, while the fluorescence emission maximum of **Pd**[**DMBil1**]-**PEG**$_{750}$ in methanol is red-shifted by 11 nm compared with that of **Pd**[**DMBil1**], the fluorescence quantum yield of the PEGylated derivative (Φ_{fl} = 1.4 × 10^{-4}) is essentially identical to that of the parent compound (Φ_{fl} = 1.3 × 10^{-4}). The phosphorescence emission maximum shows a

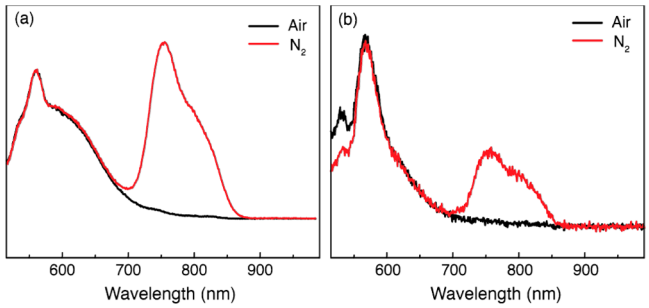

Figure 2. Emission spectra following excitation with 500 nm light of (a) **Pd**[**DMBil1**] and (b) **Pd**[**DMBil1**]-**PEG**$_{750}$ in methanol at 298 K under an atmosphere of air (black) or nitrogen (red).

much smaller red shift from 753 nm for **Pd**[**DMBil1**] to 756 nm for **Pd**[**DMBil1**]-**PEG**$_{750}$, and the phosphorescence quantum yield decreases slightly from Φ_{ph} = 1.3 × 10^{-4} for **Pd**[**DMBil1**] to Φ_{ph} = 7.8 × 10^{-5} for **Pd**[**DMBil1**]-**PEG**$_{750}$.

The emission characteristics of **Pd**[**DMBil1**]-**PEG**$_{750}$ in nitrogen-saturated PBS (pH 7.4) were also investigated; however, irradiation with 460 nm light under these conditions only resulted in one emission feature stretching from 500 to 700 nm corresponding to fluorescence (Table 1 and Figure S4). As compared with its fluorescence in methanol, the fluorescence of **Pd**[**DMBil1**]-**PEG**$_{750}$ in PBS is further red-shifted, with an emission maximum at 580 nm and a quantum yield of Φ_{fl} = 2.0 × 10^{-4} in (Table 1). Given that fluorescence quenching is a well-documented consequence of porphyrinoid self-aggregation,[33] the lack of attenuation of Φ_{fl} in PBS provides further evidence that **Pd**[**DMBil1**]-**PEG**$_{750}$ does not tend to aggregate in aqueous environments. Failure to detect phosphorescence from the PEGylated derivative in PBS may be attributed to shortening of the triplet excited-state lifetime via energy transfer to a H_2O overtone.

In prior work, we showed that air efficiently quenches the excited triplet state of **Pd**[**DMBil1**] in methanol, resulting in quenching of the biladiene's phosphorescence due to efficient energy transfer to molecular oxygen.[15] This phenomenon was also manifest in the ability of **Pd**[**DMBil1**] to photosensitize $^1O_2$ generation with an impressive quantum yield of Φ_{Δ} = 0.8, as quantified using diphenylisobenzofuran (DPBF)[34] as an $^1O_2$ probe and $[Ru(bpy)_3][PF_6]_2$ as an actinometer (Φ_{Δ} = 0.81).[35] Similarly, the phosphorescence observed for **Pd**[**DMBil1**]-**PEG**$_{750}$ in methanol under an inert atmosphere was quenched upon introduction of air (Figure 2b) to the sample. Quantification of the ability of the **Pd**[**DMBil1**]-**PEG**$_{750}$ complex to sensitize the formation of $^1O_2$ produced a quantum yield of Φ_{Δ} = 0.57 following irradiation with 550 nm light. The slight decrease in Φ_{Δ} value for the PEGylated biladiene complex may be attributed to a decrease in the O_2 diffusion rate within the immediate vicinity of the photosensitizer due to partial shielding by the PEG moiety.[36] Nonetheless, the ability of **Pd**[**DMBil1**]-**PEG**$_{750}$ to sensitize the formation of $^1O_2$ (Φ_{Δ} = 0.57) is competitive with commercial photosensitizers employed for PDT.[13]

Although **Pd**[**DMBil1**]-**PEG**$_{750}$ does not exhibit phosphorescence in PBS solutions (vide supra) this complex is capable of sensitizing the formation of $^1O_2$ under aqueous conditions. Through use of the probe singlet oxygen sensor green (SOSG)[37] and methylene blue as a reference photosensitizer (Φ_{Δ} = 0.52),[38,39] the ability of **Pd**[**DMBil1**]-**PEG**$_{750}$ to sensitize singlet oxygen was determined to be $\Phi_{\Delta} \approx$ 0.23

DOI: 10.1021/acs.inorgchem.8b01225
Inorg. Chem. XXXX, XXX, XXX−XXX

upon irradiation with 550 nm light (Table 1). The apparent attenuation of Φ_Δ in PBS relative to that in methanol is not surprising, given that detecting $^1O_2$ in aqueous environments is more challenging due to its shorter lifetime[40,41] as well as the lower solubility of oxygen in water as compared to organic solvents.[42] Importantly, however, the aqueous Φ_Δ measured for **Pd[DMBil1]-PEG$_{750}$** is high enough to enable PDT in biological samples (vide infra).

TNBC accounts for ~15−20% of diagnosed breast cancer cases and is associated with earlier relapse, higher mortality rates, and significantly decreased progression-free survival compared to non-TN breast cancers.[43] TNBC patients are unsusceptible to available targeted or hormonal therapies, because the cells in these tumors do not express the necessary surface receptors. Therefore, these patients are treated with aggressive chemotherapies and surgeries that have harmful side effects and are often unsuccessful, necessitating the development of new treatment strategies for this disease. Because of its high potency and specificity, PDT has been recognized as a promising therapeutic approach for TNBC.[44]

To evaluate the inherent toxicity of **Pd[DMBil1]-PEG$_{750}$**, TNBC MDA-MB-231 cells were treated with up to 5.0 mM **Pd[DMBil1]-PEG$_{750}$** for 48 h in the dark and then subjected to an Alamar blue cell viability assay. MDA-MB-231 cells were completely viable at **Pd[DMBil1]-PEG$_{750}$** concentrations up to 0.5 mM (Figure 4A). Further, the lethal (LD) dose required for 50% cell death was found to be LD_{50} = 1.87 mM, an exceptionally high value, which demonstrates that, in the dark, **Pd[DMBil1]-PEG$_{750}$** is biocompatible and well-tolerated by the TNBC cells.

To further demonstrate the safety profile of **Pd[DMBil1]-PEG$_{750}$** and facilitate a comparison with a set of commercially available $^1O_2$ photosensitizers that form the basis for common PDT treatments, cell viability assays were also conducted for hematoporphyrin dihydrochloride (HPDC) and isohematoporphyrin (IHP). Cell viability following treatment with up to 3.0 mM of either HPDC or IHP revealed lethal dose values of LD_{50} = 1.22 mM and LD_{50} = 0.64 mM, respectively, which are both lower than the LD_{50} obtained for **Pd[DMBil1]-PEG$_{750}$** (Figure S5). These results demonstrate that **Pd[DMBil1]-PEG$_{750}$** is less toxic than two commercially available photosensitizers, suggesting that it may be used as a photochemotherapeutic without causing off-target side effects that often limit the efficacy of PDT agents.

In an effort to assess whether **Pd[DMBil1]-PEG$_{750}$** is taken up by TNBC cells, MDA-MB-231 cells were treated with up to 1.5 mM **Pd[DMBil1]-PEG$_{750}$** for 48 h, and the cellular fluorescence was analyzed by fluorescence imaging and flow cytometry. As discussed above, **Pd[DMBil1]-PEG$_{750}$** retains the emission properties of **Pd[DMBil1]**, enabling its detection by fluorescence microscopy and flow cytometry. Fluorescence imaging revealed that **Pd[DMBil1]-PEG$_{750}$** is taken up by cells during the incubation period, as indicated by the red fluorescent signal (Figure 3). Further, flow cytometry analysis confirmed this result, as cells treated with **Pd[DMBil1]-PEG$_{750}$** experienced a twofold increase in median fluorescence intensity (MFI) compared to untreated cells (Figure S6). These results were encouraging given that cellular uptake is important for any compound to be used for PDT,[45] and they lead us to probe the efficacy of **Pd[DMBil1]-PEG$_{750}$** as a photochemotherapeutic agent.

To investigate the ability of **Pd[DMBil1]-PEG$_{750}$** to mediate PDT, MDA-MB-231 TNBC cells were treated with

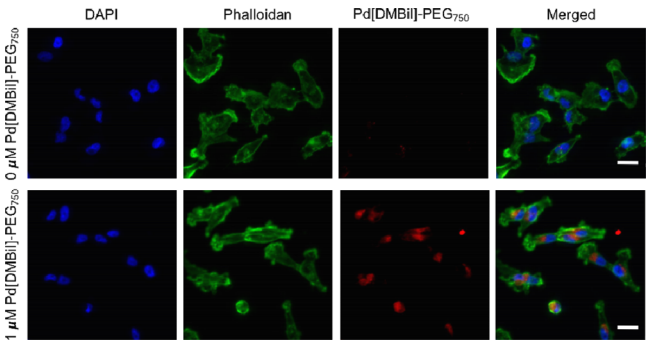

Figure 3. Fluorescence images showing **Pd[DMBil1]-PEG$_{750}$** uptake by MDA-MB-231 cells following a 24 h incubation period. Nuclei are stained blue (DAPI), F-actin in the cytoskeleton is stained green (phalloidan), and **Pd[DMBil1]-PEG$_{750}$** appears red. Scale = 25 μm.

the biladiene complex at concentrations ranging from 0 to 10.0 μM for 4 h. At each concentration surveyed, cells were irradiated (λ_{ex} > 500 nm) for either 0, 10, 20, or 30 min. Viability assays were conducted to assess cell death 16 h after irradiation. Cells incubated with **Pd[DMBil1]-PEG$_{750}$** for 24 h prior to irradiation were highly susceptible to PDT-mediated cell death compared to cells irradiated immediately after adding **Pd[DMBil1]-PEG$_{750}$**. More specifically, cells irradiated immediately following the addition of **Pd[DMBil1]-PEG$_{750}$** required concentrations of at least 1 μM and 30 min of light exposure before any loss of cell viability was observed (Figure S7). By contrast, cells incubated with **Pd[DMBil1]-PEG$_{750}$** for 24 h prior to light application were susceptible to PDT with concentrations of photosensitizer as low as 0.25 μM, and 10 μM treatment resulted in complete loss of viability (Figure 4B). This enhancement in photoinduced toxicity in cells incubated with the photosensitizer before light treatment provides further evidence of cellular uptake of **Pd[DMBil1]-PEG$_{750}$**. From these results, we also determined that the effective dose (ED) of **Pd[DMBil1]-PEG$_{750}$** required to reduce cell viability by 50% to be ED_{50} = 0.354 μM for cells incubated with the photosensitizer for 24 h and then subjected to 30 min of light exposure. The ratio of LD_{50}/ED_{50} delivers the phototoxicity index (PI) of a given photochemotherapeutic agent, which provides an indication of the potency of a photodrug in relation to its inherent dark toxicity. For **Pd[DMBil1]-PEG$_{750}$** the phototoxicity index is determined to be PI ≈ 5300, which is exceptionally high,[46] especially when compared to porphyrinoids typically employed for PDT (vide infra).

To compare the phototoxicity index of **Pd[DMBil1]-PEG$_{750}$** with those for the commercially available photosensitizers, we conducted the same photodynamic activity experiments with HPDC and IHP. Treatment of MDA-MB-231 cells with each photosensitizer for 24 h followed by a 30 min period of irradiation (λ_{ex} > 500 nm) revealed effective doses of ED_{50} = 48.65 μM for HPDC and ED_{50} = 327.56 μM for IHP (Figure S8). The LD_{50} and ED_{50} values for HPDC and IHP correlate to phototoxicity indicies of PI ≈ 25 for HPDC and PTI ≈ 2 for IHP. By comparison, the phototoxicity index of **Pd[DMBil1]-PEG$_{750}$** is quite impressive, as it is ~200 and 3000 times higher than those of HPDC and IHP, respectively.

With the realization that **Pd[DMBil1]-PEG$_{750}$** is highly potent and effective for PDT via $^1O_2$ sensitization, we sought to evaluate the mechanism by which the biladiene photo-triggers cell death. Ideally PDT will induce cellular apoptosis as

DOI: 10.1021/acs.inorgchem.8b01225
Inorg. Chem. XXXX, XXX, XXX−XXX

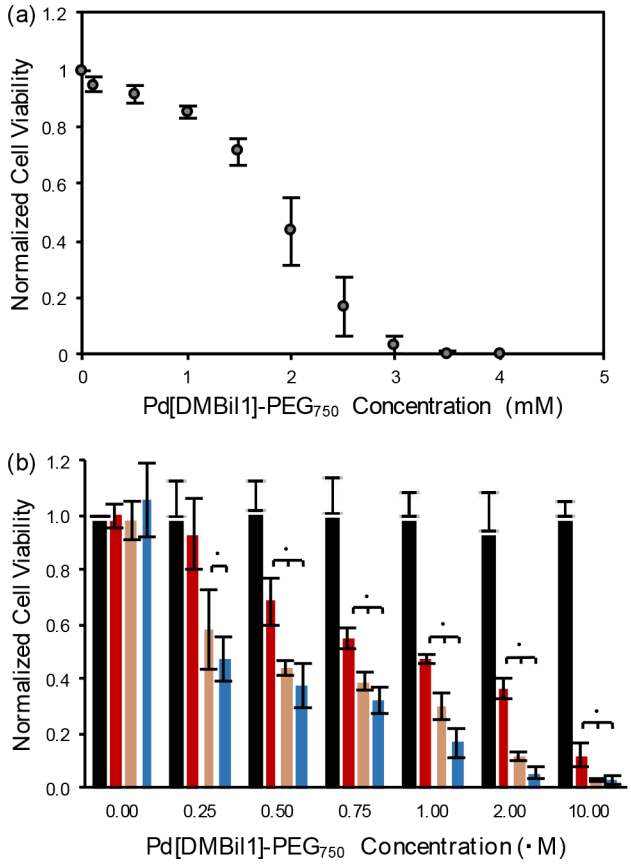

Figure 4. Normalized cell viability after incubation with **Pd[DMBil1]-PEG$_{750}$** for (a) 48 and (b) 24 h followed by light exposure for 0 (black), 10 (red), 20 (beige), or 30 (blue) min. Cells were incubated overnight post-irradiation and prior to the viability analyses. *p < 0.0001 by two-way ANOVA with post hoc Tukey-Kramer compared to 0 min light exposure for each concentration.

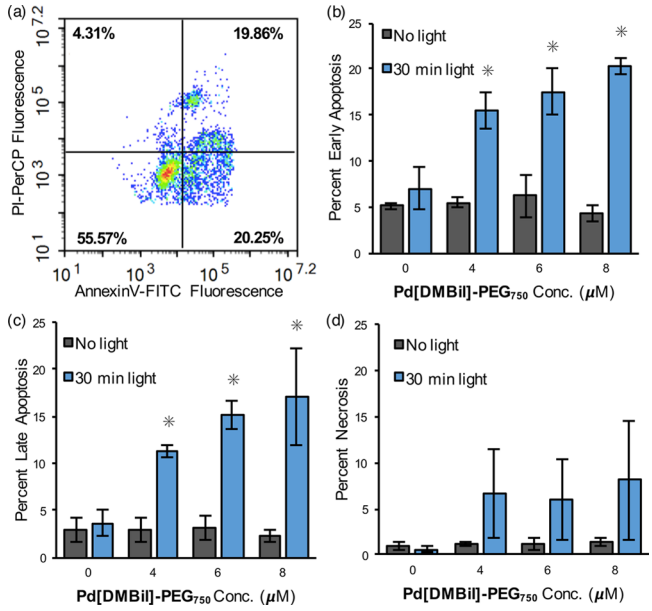

Figure 5. Apoptosis and necrosis assay after incubation with 0.0, 4.0, 6.0, or 8.0 μM of **Pd[DMBil1]-PEG$_{750}$** for 24 h, followed by light treatment for 30 min and incubation for 1 h. (A) Representative flow cytometry density plot of cells treated with 8.0 μM **Pd[DMBil1]-PEG$_{750}$**. (B–D) Flow cytometry analysis of cell populations in early apoptosis, late apoptosis, and necrosis following treatment with the photosensitizer. *p < 0.05 by t-tests compared to no light treatment for each concentration.

opposed to necrosis, as the latter can cause the release of intracellular compartments and local inflammation that can stimulate tumor growth.[47] By contrast, apoptosis is anti-inflammatory and therefore discourages disease progression.[48] To assess the mechanism by which **Pd[DMBil1]-PEG$_{750}$** photoinduces cell death, MDA-MB-231 cells were treated with 4.0, 6.0, or 8.0 μM **Pd[DMBil1]-PEG$_{750}$** for 24 h, irradiated for 30 min (λ_{ex} > 500 nm), and then incubated for 1 h prior to AnnexinV (fluorescein isothiocyanate (FITC) channel) and PI (PerCP channel) staining. Experiments in which none of the biladiene photosensitizer was added to the cells were also performed as controls. For these experiments, the MDA-MB-231 cells were treated with higher **Pd[DMBil1]-PEG$_{750}$** concentrations than in the viability experiments because we analyzed the cells only 1 h post light treatment (as opposed to overnight). Although these photosensitizer concentrations are higher than required for effective PDT, they are still more than 2 orders of magnitude lower than the LD$_{50}$ determined for **Pd[DMBil1]-PEG$_{750}$**. In these experiments, each mechanism of cell death appears in a distinct quadrant of Figure 5A depending on their level of staining. For example, live cells are negative for both FITC and PI (lower left quadrant), apoptotic cells stain positive for only FITC (lower right quadrant), late apoptotic cells stain positive for both FITC and PI (upper right quadrant), and necrotic cells stain positive for only PI (upper left quadrant).

The results of the apoptosis and necrosis assay show that PDT with **Pd[DMBil1]-PEG$_{750}$** induces primarily apoptotic cell death and that the percentage of apoptotic cells increases with higher photosensitizer concentrations (Figures 5 and S9). The maximum amount of positively stained cells resulted from treatment with 8.0 μM **Pd[DMBil1]-PEG$_{750}$**. The average of three separate assays showed that 20.21% of cells were positive for early apoptosis, 17.08% of cells were positive for late apoptosis, and 8.17% of cells stained positive for necrosis only. Alternatively, cells that did not undergo light treatment experienced only minimal cell death by any mechanism. These results demonstrate that almost half of the total cell populations treated with **Pd[DMBil1]-PEG$_{750}$** that are exposed to light for 30 min experience primarily apoptotic cell death, and ~82% of the cells killed by the phototreatment expire via apoptosis rather than necrosis. Given that apoptosis is much preferred over necrosis for cancer treatment, these results make **Pd[DMBil1]-PEG$_{750}$** even more attractive as a potential photosensitizer for use in PDT.

CONCLUSIONS AND FUTURE DIRECTIONS

The development of new biologically compatible $^1O_2$ sensitizers for use as PDT agents remains a topic of significant interest,[49] given the benefits that phototherapeutics can hold over more conventional treatment options for certain cancers. Despite these advantages and the fact that PDT has been approved to treat cancers of the skin, head, neck, digestive system, ovaries, prostate, bladder, lungs, breast, and brain,[2] its adoption as a mainstream cancer treatment has been hampered by a general lack of $^1O_2$ photosensitizers that are efficient, biologically tolerated, and pose minimal side effects and toxicity in the dark. In this work we described our efforts to address these shortcomings through development of a water-

DOI: 10.1021/acs.inorgchem.8b01225
Inorg. Chem. XXXX, XXX, XXX−XXX

soluble dimethylbiladiene derivative (**Pd[DMBil1]-PEG$_{750}$**) that can sensitize the formation of singlet O_2 with high quantum yield under biologically relevant conditions.

Preparation of the **Pd[DMBil1]-PEG$_{750}$** complex was accomplished in two straightforward, high-yielding steps from the parent palladium dimethylbiladiene complex, and photophysical studies revealed that PEGylation of the tetrapyrrole core has little effect on the electronic properties of the parent **Pd[DMBil1]** complex. In the absence of oxygen, **Pd[DMBil1]-PEG$_{750}$** displays both fluorescence and phosphorescence when dissolved in methanol. Notably, the triplet emission signal is completely quenched upon introduction of air to the sample due to efficient sensitization of $^1O_2$ with a quantum yield of Φ_Δ = 0.57, which is competitive with traditional sensitizers employed for PDT, including Photofrin.

Pd[DMBil1]-PEG$_{750}$ is highly soluble in water as well as in biological media. Measurement of the photophysical properties of **Pd[DMBil1]-PEG$_{750}$** in pH 7.4 PBS solutions showed that the complex does not aggregate and can photosensitize $^1O_2$ under aqueous conditions. The efficacy of **Pd[DMBil1]-PEG$_{750}$** as a photochemotherapeutic agent was assessed using TNBC MDA-MB-231 cells, which readily take up the biladiene construct as evidenced by fluorescence microscopy and flow cytometry. In the dark, the **Pd[DMBil1]-PEG$_{750}$** complex is extremely well-tolerated by the TNBC cells and has an LD_{50} of 1.87 mM. By contrast, the PEGylated palladium biladiene is an exceptionally potent photochemotherapeutic agent, as the effective dose of this complex required to reduce the TNBC viability by 50% was determined to be ED_{50} = 0.354 μM after 30 min of irradiation. Consideration of both the ED_{50} and LD_{50} metrics delivers the PI of **Pd[DMBil1]-PEG$_{750}$**, which is a benchmark of the efficacy of a photochemotherapeutic agent in relation to its inherent dark toxicity. **Pd[DMBil1]-PEG$_{750}$** has a remarkably high phototoxicity index of PI $\approx$ 5300. This value dwarfs those determined for molecular surrogates of existing commercial PDT agents, as HPDC and IHP were found to have photoxicity indices of just PI $\approx$ 25 and PI $\approx$ 2, respectively.

Since comparison of the PI of **Pd[DMBil1]-PEG$_{750}$** to those for common porphyrin-based PDT models suggests that the linear palladium(II) tetrapyrrole can be a vastly superior photochemotherapeutic agent, the mechanism by which **Pd[DMBil1]-PEG$_{750}$** phototriggers TNBC cell death was probed. Cell death assays show that PDT with **Pd[DMBil1]-PEG$_{750}$** induces primarily apoptotic cell death as opposed to necrosis, as ~82% of the TNBC cells that die as a result of PDT do so via apoptosis. This finding serves to further distinguish **Pd[DMBil1]-PEG$_{750}$** as a photochemotherapeutic agent, since apoptosis is much preferred over necrosis for cancer treatments, because the latter can result in local inflammation that stimulates tumor growth.

When viewed as a whole, this study demonstrates that **Pd[DMBil1]-PEG$_{750}$** holds promise as a photochemotherapeutic agent and should warrant further investigation as a PDT photosensitizer for treatment of cancers including TNBC. From a broader perspective, while macrocyclic tetrapyrroles such as porphyrins and phthalocyanines have been well-studied as potential PDT agents, this work demonstrates that properly engineered linear oligopyrrole complexes may represent a privileged class of $^1O_2$ sensitizers for the treatment of human disease. Building off our findings that **Pd[DMBil1]-PEG$_{750}$** is well-tolerated by TNBC cells and is a potent $^1O_2$ sensitizer, future efforts will be focused on pushing the absorption envelope for this and related complexes further into the therapeutic window, either via modulation of the tetrapyrrole core or by using photon upconversion strategies, to better enable the use of such platforms in tissue and animal models.

■ ASSOCIATED CONTENT

Supporting Information

The Supporting Information is available free of charge on the ACS Publications Web site. The Supporting Information is available free of charge on the ACS Publications website at DOI: 10.1021/acs.inorgchem.8b01225.

Experimental procedures, additional **Pd[DMBil1]-PEG$_{750}$** characterization data, and photodynamic therapy data (PDF)

■ AUTHOR INFORMATION

Corresponding Authors

*E-mail: emilyday@udel.edu. (E.S.D.)
*E-mail: joelr@udel.edu. (J.R.)

ORCID

Rachel S. Riley: 0000-0002-3267-5403
Joel Rosenthal: 0000-0002-6814-6503

Author Contributions

$^\perp$These authors contributed equally. The manuscript was written through contributions of all authors. All authors have given approval to the final version of the manuscript.

Notes

The authors declare no competing financial interest.

■ ACKNOWLEDGMENTS

A Strategic Initiatives Grant from the Univ. of Delaware (UD) Research Foundation and the State of Delaware Federal Research and Development Grant Program (16A00471) supported portions of this work. This work was also supported through NSF CAREER Award Nos. CHE1352120 and NIH P20GM104316. NMR and other data were acquired at UD using instrumentation obtained with assistance from the NSF and NIH (NSF-MIR 0421224, NSF-MIR 1048367, NSF-CRIF MU CHE-0840401 and CHE-0541775, NIH P20 RR017716). R.S.R. received support from the Univ. of Delaware Graduate Fellowship and from the American Association of Univ. Women.

■ REFERENCES

(1) Knoll, J. D.; Albani, B. A.; Turro, C. New Ru(II) Complexes for Dual Photoreactivity: Ligand Exchange and $^1O_2$ Generation. *Acc. Chem. Res.* **2015**, *48*, 2280−2287.

(2) Agostinis, P.; Berg, K.; Cengel, K. A.; Foster, T. H.; Girotti, A. W.; Gollnick, S. O.; Hahn, S. M.; Hamblin, M. R.; Juzeniene, A.; Kessel, D.; Korbelik, M.; Moan, J.; Mroz, P.; Nowis, D.; Piette, J.; Wilson, B. C.; Golab, J. Photodynamic Therapy of Cancer: An Update. *Ca-Cancer J. Clin.* **2011**, *61*, 250−281.

(3) Ozog, D. M.; Rkein, A. M.; Fabi, S. G.; Gold, M. H.; Goldman, M. P.; Lowe, N. J.; Martin, G. M.; Munavalli, G. S. Photodynamic Therapy: A Clinical Consensus Guide. *Dermatol. Surg.* **2016**, *42*, 804−827.

(4) Wang, H.; Xu, Y.; Shi, J.; Gao, X.; Geng, L. *Photodermatol., Photoimmunol. Photomed.* **2015**, *31*, 44−53.

(5) Miltenburg, N. C.; Boogerd, W. Chemotherapy-Induced Neuropathy: A Comprehensive Survey. *Cancer Treat. Rev.* **2014**, *40*, 872−882.

DOI: 10.1021/acs.inorgchem.8b01225
Inorg. Chem. XXXX, XXX, XXX−XXX

(6) Love, R. R.; Leventhal, H.; Easterling, D. V.; Nerenz, D. R. Side Effects and Emotional Distress During Cancer Chemotherapy. *Cancer* **1989**, *63*, 604−612.
(7) Lau, T. K. H.; Yip, C. H. W.; Yeo, W. State of the Art Antiemetic Therapy for Cancer Patients. *Curr. Oncol. Rep.* **2016**, *18*, 1−13.
(8) Armstrong, G. T.; Stovall, M.; Robison, L. L. Long-Term Effects of Radiation Exposure among Adult Survivors of Childhood Cancer: Results from the Childhood Cancer Survivor Study. *Radiat. Res.* **2010**, *174*, 840−850.
(9) Khan, H. A.; Alhomida, A. S. A Review of the Logistic Role of *l*-carnitine in the Management of Radiation Toxicity and Radiotherapy Side Effects. *J. Appl. Toxicol.* **2011**, *31*, 707−713.
(10) Nowis, D.; Stoklosa, T.; Legat, M.; Issat, T.; Jakobisiak, M.; Golab, J. The Influence of Photodynamic Therapy on the Immune Response. *Photodiagn. Photodyn. Ther.* **2005**, *2*, 283−298.
(11) Castano, A. P.; Mroz, P.; Hamblin, M. R. Photodynamic Therapy and Anti-Tumor Immunity. *Nat. Rev. Cancer* **2006**, *6*, 535−545.
(12) Bonnett, R. Photosensitizers of the Porphyrin and Phthalocyanine Series for Photodynamic Therapy. *Chem. Soc. Rev.* **1995**, *24*, 19−33.
(13) Ormond, A. B.; Freeman, H. S. Dye Sensitizers for Photodynamic Therapy. *Materials* **2013**, *6*, 817−840.
(14) O'Connor, A. E.; Gallagher, W. M.; Byrne, A. T. Porphyrin and Nonporphyrin Photosensitizers in Oncology: Preclinical and Clinical Advances in Photodynamic Therapy. *Photochem. Photobiol.* **2009**, *85*, 1053−1074.
(15) Potocny, A. M.; Pistner, A. J.; Yap, G. P. A.; Rosenthal, J. Electrochemical, Spectroscopic, and $^1O_2$ Sensitization Characteristics of Synthetically Accessible Linear Tetrapyrrole Complexes of Palladium and Platinum. *Inorg. Chem.* **2017**, *56*, 12703−12711.
(16) Li, W.; Zhan, P.; De Clercq, E.; Lou, H.; Liu, X. Current Drug Research on PEGylation with Small Molecular Agents. *Prog. Polym. Sci.* **2013**, *38*, 421−444.
(17) Greenwald, R. B.; Choe, Y. H.; McGuire, J.; Conover, C. D. Effective Drug Delivery by PEGylated Drug Conjugates. *Adv. Drug Delivery Rev.* **2003**, *55*, 217−250.
(18) Working, P. K.; Newman, M. S.; Johnson, J.; Cornacoff, J. B. In *Poly(ethylene glycol) Chemistry and Biological Applications;* Harris, J. M., Zalipsky, S., Eds.; American Chemical Society: Washington, DC, 1997; pp 45−57.
(19) Powell, G. M. In *Handbook of Water Soluble Gums and Resins;* Davidson, R. L., Crawford, H. B., Williams, J., Eds.; McGraw-Hill: New York, 1980; pp 18-8−18-14.
(20) Pistner, A. J.; Pupillo, R. C.; Yap, G. P. A.; Lutterman, D. A.; Ma, Y. Z.; Rosenthal, J. Electrochemical, Spectroscopic and Singlet Oxygen Sensitization Characteristics of 10,10-Dimethylbiladiene Complexes of Zinc and Copper. *J. Phys. Chem. A* **2014**, *118*, 10639−10648.
(21) Pistner, A. J.; Yap, G. P.; Rosenthal, J. A Tetrapyrrole Macrocycle Displaying a Multielectron Redox Chemistry and Tunable Absorbance Profile. *J. Phys. Chem. C* **2012**, *116*, 16918−1692.
(22) Pistner, A. J.; Lutterman, D. A.; Ghidiu, M. J.; Ma, Y. Z.; Rosenthal, J. Synthesis, Electrochemistry and Photophysics of a Family of Phlorin Macrocycles that Display Cooperative Fluoride Binding. *J. Am. Chem. Soc.* **2013**, *135*, 6601−6607.
(23) Pistner, A. J.; Lutterman, D. A.; Ghidiu, M. J.; Walker, E.; Yap, G. P. A.; Rosenthal, J. Factors Controlling the Spectroscopic Properties and Supramolecular Chemistry of an Electron Deficient 5,5-Dimethylphlorin Architecture. *J. Phys. Chem. C* **2014**, *118*, 14124−14132.
(24) Bhupathiraju, N. V. S. D. K.; Rizvi, W.; Batteas, J. D.; Drain, C. M. Fluorinated Porphyrinoids as Efficient Platforms for New Photonic Materials, Sensors, and Therapeutics. *Org. Biomol. Chem.* **2016**, *14*, 389−408.
(25) Costa, J. I. T.; Tomé, A. C.; Neves, M. G. P. M. S.; Cavaleiro, J. A. S. 5,10,15,20-tetrakis(pentafluorophenyl)porphyrin: a Versatile Platform to Novel Porphyrinic Materials. *J. Porphyrins Phthalocyanines* **2011**, *15*, 1116−1133.
(26) Rosenthal, J.; Schuster, D. I. The Anomalous Reactivity of Fluorobenzene in Electrophilic Aromatic Substitution and Related Phenomena. *J. Chem. Educ.* **2003**, *80*, 679−690.
(27) Han, S.-Y.; Kim, Y.-A. Recent Development of Peptide Coupling Reagents in Organic Synthesis. *Tetrahedron* **2004**, *60*, 2447−2467.
(28) Albeiicio, F.; Chinchilla, R.; Dodsworth, D. J.; Nájera, C. New Trends in Peptide Coupling Reagents. *Org. Prep. Proced. Int.* **2001**, *33*, 203−313.
(29) Leighton, P.; Cowan, J. A.; Abraham, R. J.; Sanders, J. K. M. Geometry of Porphyrin−Porphyrin Interactions. *J. Org. Chem.* **1988**, *53*, 733−740.
(30) Reddi, E.; Jori, G. Steady-State and Time-Resolved Spectroscopic Studies of Photodynamic Sensitizers: Porphyrins and Phthalocyanines. *Rev. Chem. Intermed.* **1988**, *10*, 241−268.
(31) Matsubara, S.; Kunieda, M.; Wada, A.; Sasaki, S.; Tamiaki, H. Visible and Near-Infrared Spectra of Chlorosomal Zinc Chlorin Self-Aggregates Dependent on Their Peripheral Substituents at the 8-position. *J. Photochem. Photobiol., A* **2016**, *330*, 195−199.
(32) White, W. I. In *The Porphyrins;* Dolphin, D., Ed.; Academic Press: New York, 1978; Vol. *5*: Physical Chemistry, Part C, pp 303−339.
(33) Siggel, U.; Bindig, U.; Endisch, C.; Komatsu, T.; Tsuchida, E.; Voigt, J.; Fuhrhop, J.-H. Photophysical and Photochemical Properties of Porphyrin Aggregates. *Ber. Bunsenges. Phys. Chem.* **1996**, *100*, 2070−2075.
(34) Young, R. H.; Wehrly, D.; Martin, R. L. Solvent Effects in Dye-Sensitized Photooxidation Reactions. *J. Am. Chem. Soc.* **1971**, *93*, 5774−5779.
(35) Bhattacharyya, K.; Das, P. K. Quantitative Aspects of All-Trans-Retinol Singlet and Triplet Quenching by Oxygen. *Chem. Phys. Lett.* **1985**, *116*, 326−332.
(36) Li, S. P.-Y.; Lau, C. T.-S.; Louie, M.-W.; Lam, Y.-W.; Cheng, S. H.; Lo, K. K.-W. Mitochondria-Targeting Cyclometalated Iridium(III) − PEG Complexes with Tunable Photodynamic Activity. *Biomaterials* **2013**, *34*, 7519−7532.
(37) Ragàs, X.; Jiménez-Banzo, A.; Sánchez-García, D.; Batllori, X.; Nonell, S. Singlet Oxygen Photosensitization by the Fluorescent Probe Singlet Oxygen Sensor Green. *Chem. Commun.* **2009**, *20*, 2920−2922.
(38) Nemoto, M.; Kokubun, H.; Koizumi, M. Determination of the S*−T Transition Probabilities of Some Xanthene and Thiazine Dyes on the Basis of T-Energy Transfer. II. Results in the Aqueous Solution. *Bull. Chem. Soc. Jpn.* **1969**, *42*, 2464−2470.
(39) Usui, Y.; Kamogawa, K. A Standard System to Determine the Quantum Yield of Singlet Oxygen Formation in Aqueous Solution. *Photochem. Photobiol.* **1974**, *19*, 245−247.
(40) Egorov, S. Y.; Kamalov, V. F.; Koroteev, N. I.; Krasnovsky, A. A., Jr.; Toleutaev, B. N.; Zinukov, S. V. Rise and Decay Kinetics of Photosensitized Singlet Oxygen Luminescence in Water. Measurements with Nanosecond Time-Correlated Single Photon Counting Technique. *Chem. Phys. Lett.* **1989**, *163*, 421−424.
(41) Cheng, C.-C.; Wu, G.-R.; Chiou, C.-S.; Yu, J.-K.; Chou, P.-T. Time-Resolved Thermal Lensing Studies on Metastable Species. *J. Chin. Chem. Soc.* **2003**, *50*, 31−39.
(42) Quaranta, M.; Murkovic, M.; Klimant, I. A New Method to Measure Oxygen Solubility in Organic Solvents Through Optical Oxygen Sensing. *Analyst* **2013**, *138*, 6243−6245.
(43) Griffiths, C.; Olin, J. Triple Negative Breast Cancer: A Brief Review of its Characteristics and Treatment Options. *J. Pharm. Pract.* **2012**, *25*, 319−323.
(44) Shemesh, C.; Hardy, C.; Yu, D.; Fernandez, B.; Zhang, H. Indocyanine Green Loaded Liposome Nanocarriers for Photodynamic Therapy Using Human Triple Negative Breast Cancer Cells. *Photodiagn. Photodyn. Ther.* **2014**, *11*, 193−203.
(45) Castano, A.; Demidova, T.; Hamblin, M. Mechanisms in Photodynamic Therapy: Part One−Photosensitizers, Photochemistry and Cellular Localization. *Photodiagn. Photodyn. Ther.* **2004**, *1*, 279−293.

DOI: 10.1021/acs.inorgchem.8b01225
Inorg. Chem. XXXX, XXX, XXX−XXX

(46) Mroz, P.; Yaroslavsky, A.; Kharkwal, G. B.; Hamblin, H. Cell Death Pathways in Photodynamic Therapy of Cancer. *Cancers* **2011**, *3*, 2516−2539.
(47) Melamed, J.; Edelstein, R.; Day, E. Elucidating the Fundamental Mechanisms of Cell Death Triggered by Photothermal Therapy. *ACS Nano* **2015**, *9*, 6−11.
(48) Albani, B. A.; Peña, B.; Leed, N. A.; de Paula, N. A. B. G.; Pavani, C.; Baptista, M. S.; Dunbar, K. R.; Turro, C. Marked Improvement in Photoinduced Cell Death by a New Tris-heteroleptic Complex with Dual Action: Singlet Oxygen Sensitization and Ligand Dissociation. *J. Am. Chem. Soc.* **2014**, *136*, 17095−17101.
(49) Loftus, L. M.; White, J. K.; Albani, B. A.; Kohler, L.; Kodanko, J. J.; Thummel, R. P.; Dunbar, K. R.; Turro, C. New Ru^{II} for Dual Activity: Photoinduced Ligand Release and $^1O_2$ Production. *Chem. - Eur. J.* **2016**, *22*, 3704−3708.

DOI: 10.1021/acs.inorgchem.8b01225
Inorg. Chem. XXXX, XXX, XXX−XXX